

Tropical Fermat-Weber Points over Spaces of M -Ultrametrics

Shelby Cox^{1†}, John Sabol^{2†}, Roan Talbut^{3†}, Ruriko Yoshida^{2*}

¹The Max Planck Institute for Mathematics in the Sciences, Inselstraße 22, Leipzig, 04103, Germany.

²Operations Research Department, Naval Postgraduate School, 1411 Cunningham Road, Monterey, 93943, CA, USA.

³Mathematics Department, Imperial College London, South Kensington Campus, London, SW7 2AZ, UK.

*Corresponding author(s). E-mail(s): ryoshida@nps.edu;

Contributing authors: spcox@umich.edu; john.sabol@nps.edu;

r.talbut21@imperial.ac.uk;

†These authors contributed equally to this work.

Abstract

We extend reconstruction methods for phylogenetic trees to ultrametrics of arbitrary matroids and study the stability of these data analysis methods in the combinatorial spirit of Andreas Dress. In particular, we generalize Atteson's work on the safety radius of phylogenetic reconstruction methods, as well as Gascuel and Steel's work on the stochastic safety radius, to arbitrary matroids. We also show that although the tropical Fermat-Weber points of an M -ultrametric sample are generally not contained in the space of M -ultrametrics, the intersection between the Fermat-Weber set and the space of M -ultrametrics is non-empty.

Keywords: Matroids, Max-Plus Algebra, Phylogenomics, Tropical Geometry

Dedicated to Andreas Dress

1 Introduction

Andreas Dress was a pioneer at the intersection of mathematics and evolutionary biology. In particular, he made significant contributions to the combinatorics of phylogenetic trees (for example, (Dress et al. 2014)). A phylogenetic tree is a metric tree with non-negatively weighted edges, which is often used to represent evolutionary relationships between taxa. It is well known that the space of phylogenetic trees with p leaves is the Dressian $\text{Dr}(2, p)$. In (Dress et al. 2005), Andreas Dress studied *ultrametrics*, or equivalently, *equidistant trees*, which are rooted phylogenetic trees whose total branch length from the root to each leaf is the same for all p leaves. In 2006, Ardila and Klivans showed that the space of ultrametrics is the Bergman fan associated with the matroid of the complete graph on p vertices (Ardila and Klivans 2006).

In phylogenetics, one of the main tasks is to reconstruct a phylogenetic tree from an alignment. A *distance-based method* for phylogenetic tree reconstruction is a map which takes a dissimilarity metric as input data, and maps onto the space of phylogenetic trees. Distance-based reconstruction methods were generalized to Bergman fans of arbitrary matroids by Ardila (2004) via tropical projection, and studied by Bernstein (2020). There, the points of the Bergman fan of M are called M -ultrametrics.

In this paper, we study the tropical projection of *tropical Fermat-Weber points* to spaces of M -ultrametrics via the map defined in Theorem 5. Fermat-Weber points are a generalization of the median to arbitrary metric spaces. *Tropical* Fermat-Weber points are Fermat-Weber points in the tropical projective torus, equipped with the standard tropical metric. It is known that in this case, even if all observations are M -ultrametrics, the tropical Fermat-Weber points are not, in general, M -ultrametrics (Lin et al. 2017); for more on tropical Fermat-Weber points, see Sabol et al. (2024). In Theorem 12, we show that if all observations are M -ultrametrics, then the intersection of the set of tropical Fermat-Weber points and the space of M -ultrametrics is not empty, and that it is equal to the projection of the Fermat-Weber points onto the space of M -ultrametrics.

In practice, observed data are usually not M -ultrametrics due to noise in the observations. To quantify the maximum error under which projected tropical Fermat-Weber points are stable, we extend the definition of *safety radius* for phylogenetic reconstruction, originally given by Atteson in (Atteson 1999), to the projection of the set of all tropical Fermat-Weber points to the space of M -ultrametrics. In Theorem 17, we show that this M -ultrametric reconstruction method has safety radius $1/2$ for any matroid, which is the maximum possible.

We also consider the influence of stochastic error, for which we define the *Fermat-Weber M -ultrametric stochastic safety radius* (Theorem 18), extending the definition of stochastic safety radius for phylogenetic construction given by Gascuel and Steel in (Gascuel and Steel 2016). In Theorem 19, we show that our generalized stochastic safety radius is always non-zero. We end with some computational experiments demonstrating the FW M -ultrametric safety radius for a sample from a particular Bergman fan under additive Gaussian noise, and a summary of experiments for all matroids on 8 elements. Our results suggest that in practice our bound for the FW M -ultrametric safety radius is very conservative, which aligns with previous observations in the case of phylogenetic trees (Gascuel and Steel 2016).

The paper is structured as follows. [Section 2](#) reviews the necessary background in phylogenetics and tropical geometry, and connects these areas through the definition of the M -ultrametric safety radius ([Theorem 8](#)). In [Section 3](#), we determine the safety radius of the procedure which takes a finite sample of M -ultrametrics to the projection of its tropical Fermat-Weber points. Finally, in [Section 4](#), we prove bounds on the stochastic safety radius and discuss experimental results.

Notation

Throughout this paper we denote $[p] := \{1, \dots, p\}$ for a positive integer p . We use $\mathbf{1}_U$ to denote the zero-one vector with support U , and write $x_a + y_a$ as $(x + y)_a$. For a point $w \in \mathbb{R}^q$, we use the notation $\text{argmax}_{e \in [q]} w_e = \{e \in [q] : w_e = \max_{f \in [q]} w_f\}$. We use \mathbb{I}_q to denote the $q \times q$ identity matrix, and $\mathbb{P}(A)$ for the probability of event A .

2 Safety Radius for M -Ultrametrics

In this section, we recall the tropical projection onto the space of M -ultrametrics, and we define its *safety radius*. We begin by reminding readers of some background on phylogenetic trees.

2.1 Phylogenetics

A phylogenetic tree on p leaves is a rooted tree with non-negatively weighted edges which represents the evolutionary history of a set of p taxa or species. Its internal vertices are unlabeled, and its p leaves are labeled bijectively by the elements of $[p]$. We further assume the root has degree at least two, and all other internal vertices have degree at least three. We denote by $E(T)$ the edges of the phylogenetic tree T . An edge of T is an *internal edge* if neither endpoint is a leaf. The *space of all phylogenetic trees on p leaves* is denoted \mathcal{T}_p .

The *topology* of a phylogenetic tree T , which we denote by $\tau(T)$, is the underlying unweighted, leaf-labeled graph of T . A tree topology is *binary* if the root has degree two, and every other non-leaf vertex has degree three. For example, of the 26 distinct tree topologies with four leaves, 15 topologies are binary.

A *distance-based phylogenetic reconstruction method* (or *distance-based method*) takes as input estimated pairwise evolutionary distances among p taxa, and outputs a phylogenetic tree on p leaves. For further information on how these distances are obtained in practice, see ([Semple and Steel 2003](#)). This set of estimated pairwise distances forms a *dissimilarity matrix*, that is, a symmetric non-negative $p \times p$ matrix, $D = [d_{ij}]$, where d_{ij} encodes the evolutionary distance between taxa $i, j \in [p]$. Note that D is not necessarily a metric, since we do not assume that it satisfies the triangle inequality. We denote the *set of $p \times p$ dissimilarity matrices* by \mathcal{D}_p .

The *tree metric* associated to a phylogenetic tree T is the dissimilarity matrix whose (i, j) entry records the length of the unique path in T from leaf i to leaf j . Each tree metric arises from a unique tree ([Semple and Steel 2003](#), Theorem 7.2.8). Thus, we identify the space of phylogenetic trees \mathcal{T}_p with the subset of dissimilarity

matrices that arise as tree metrics. With this notation, a distance-based phylogenetic reconstruction method is simply a function $\phi : \mathcal{D}_p \rightarrow \mathcal{T}_p$.

An *equidistant tree* on p leaves is a phylogenetic tree such that the distance from the root to any leaf is the same. Such trees appear in phylogenetics under the molecular clock assumption, which asserts that all lineages evolve at roughly equal rates. The tree metric of an equidistant tree is also known as an ultrametric (Buneman 1974). We use \mathcal{U}_p to refer to the space of equidistant trees on p leaves, or equivalently to the subset of $p \times p$ dissimilarity matrices that arise as the tree metric of an equidistant tree.

In practice, dissimilarity measures are estimated from data which are noisy or incomplete, resulting in dissimilarity matrices that typically do not satisfy the four point condition. While it is impossible to recover a tree metric exactly from its noisy dissimilarity matrix, the primary concern of phylogenetic reconstruction is recovering the correct tree topology. Therefore, one asks: when does a distance-based method produce a tree with the same topology as T , given noisy input $D = D_T + \epsilon$?

The *safety radius*, introduced by Atteson (1999), quantifies the amount of noise a distance-based method can tolerate. The tolerance for a given tree T depends on the minimum edge length in T .

Definition 1 (Safety radius, (Atteson 1999)) *Let $l(e)$ denote the length of edge e for $e \in E(T)$. A distance-based reconstruction method $\phi : \mathcal{D}_p \rightarrow \mathcal{T}_p$ has safety radius s if for every binary tree $T \in \mathcal{T}_p$, and every dissimilarity matrix $D \in \mathcal{D}_p$ such that*

$$\|D_T - D\|_\infty < s \cdot \min_{e \in E(T)} l(e),$$

the tree $\phi(D)$ has topology $\tau(T)$.

Atteson also shows that the safety radius of any distance-based method is at most $1/2$ (Lemma 3, Atteson (1999)). In Theorem 8, we will adapt this safety radius to ultrametrics of arbitrary matroids.

2.2 M -Ultrametrics

Our goal in this section is to generalize the notion of safety radius to M -ultrametric reconstruction methods. An *M -ultrametric reconstruction method* is a function that takes as input a point in $\mathbb{R}^q / \mathbb{R}1$ and outputs an M -ultrametric. The reconstruction method we study is a nearest point map under the tropical symmetric metric to the space of M -ultrametrics. We begin with the relevant background on matroids and tropical geometry. We assume that the reader has some familiarity with these topics; for further details, we refer the reader to (Joswig 2021).

M -ultrametrics are a generalization of ultrametrics to arbitrary matroids as introduced by Ardila (2004). We refer to the set of all M -ultrametrics for the matroid M as the *space of M -ultrametrics*.

Definition 2 *Let M be a matroid on ground set $[q]$. The space of M -ultrametrics, denoted \mathcal{U}_M , is the set of all $w \in \mathbb{R}^q$ such that for every circuit C , $\text{argmax}_{e \in C} w_e$ has cardinality at least two.*

The space of M -ultrametrics can be endowed with the structure of a polyhedral fan, the coarsest such fan structure being the Bergman fan. Since \mathcal{U}_M is the underlying set of the Bergman fan $\tilde{\mathcal{B}}(M)$, we sometimes refer to the set \mathcal{U}_M as a Bergman fan. The fan structure we consider on \mathcal{U}_M is the nested set fan on connected flats as described in (Bernstein 2020); see also (Feichtner and Sturmfels 2005). We denote this fan structure by $\tilde{N}(M)$. Through the rest of this paper, we make the usual assumption that M is connected for notational ease.

Recall that a *nested set*, \mathcal{S} , is a set of connected flats such that for all pairwise incomparable $F_1, \dots, F_r \in \mathcal{S}$, the closure of their union, $\overline{F_1 \cup \dots \cup F_r}$, is disconnected. As in (Bernstein 2020), we further require that every nested set contains $[q]$. The cones of $\tilde{N}(M)$ are in bijection with the collection of nested sets, and we denote the cone corresponding to a nested set \mathcal{S} by $K_{\mathcal{S}}$. For each \mathcal{S} , we have

$$K_{\mathcal{S}} := \{\mu \mathbf{1} + \sum_{F \in \mathcal{S}} -\lambda_F \mathbf{1}_F \mid \lambda_F \geq 0, \mu \in \mathbb{R}\}. \quad (1)$$

We will denote by $\text{relint } K_{\mathcal{S}}$ the relative interior of $K_{\mathcal{S}}$, which is the interior of $K_{\mathcal{S}}$ as a subset of the affine span of $K_{\mathcal{S}}$. The boundary of $K_{\mathcal{S}}$ is $\partial K_{\mathcal{S}} := K_{\mathcal{S}} \setminus \text{relint } K_{\mathcal{S}}$.

In this paper, we use an alternative characterization of the cones of $\tilde{N}(M)$, which is described in terms of the argmax sets for each circuit. The *argmax fan* structure on \mathcal{U}_M consists of the cones $\{K^w : w \in \mathcal{U}_M\}$, where:

$$K^w := \overline{\{u \in \mathcal{U}_M : \text{for all circuits } C \text{ of } M, \underset{e \in C}{\text{argmax}} u_e = \underset{e \in C}{\text{argmax}} w_e\}}.$$

It is clear that each K^w is a cone, and $K^w \subseteq K^{w'}$ if and only if, for all circuits C of M , $\underset{e \in C}{\text{argmax}} w'_e \subseteq \underset{e \in C}{\text{argmax}} w_e$, with a strict inclusion on the left if and only if there is a strict inclusion on the right for at least one circuit. We now show that the argmax fan is exactly the nested set fan.

Lemma 3 *Let $K_{\mathcal{S}}$ be a cone in the nested set fan $\tilde{N}(M)$ with $w \in \text{relint } K_{\mathcal{S}}$. Then $K_{\mathcal{S}} = K^w$. Furthermore, if $K_{\mathcal{S}'}$ is another cone in the nested set fan $\tilde{N}(M)$ with $w' \in \text{relint } K_{\mathcal{S}'}$, then*

$$K_{\mathcal{S}} \subseteq K_{\mathcal{S}'} \iff K^w \subseteq K^{w'}. \quad (2)$$

Proof Given any nested set \mathcal{S} , and any $w \in \text{relint } K_{\mathcal{S}}$, the data $\{(C, \underset{e \in C}{\text{argmax}} w_e) : C \text{ is a circuit of } M\}$ is determined by \mathcal{S} . Specifically, we claim that for any circuit C , $\underset{e \in C}{\text{argmax}} w_e = C \setminus \cup_{C \not\subseteq F \in \mathcal{S}} F =: C'$.

First, we show that C' is not empty. Suppose otherwise, and let F_1, \dots, F_m be a set of connected flats covering C , and satisfying $C \not\subseteq F \in \mathcal{S}$. Without loss of generality, we may assume that F_1, \dots, F_m are pairwise incomparable. Let $F = \overline{F_1 \cup \dots \cup F_m}$. Since each flat is connected and intersects C non-trivially, F is connected. But this contradicts the assumption that \mathcal{S} is a nested set. Therefore, C' is non-empty. Moreover, $\underset{e \in C}{\text{argmax}} w_e = C'$. To see this, recall that $w = \sum_{F \in \mathcal{S}} -\lambda_F \mathbf{1}_F$, with $\lambda_F > 0$ for all F (as w is in the relative interior of $K_{\mathcal{S}}$). For all $e, e' \in C'$ and $f \in C \setminus C'$, $w_e = w_{e'} > w_f$. Thus, $\underset{e \in C}{\text{argmax}} w_e = C'$.

Now consider $w \in \mathcal{U}_M$. We will show there is a nested set \mathcal{S} so that $K^w = K_{\mathcal{S}}$. We just showed that $\tilde{N}(M)$ refines the argmax fan structure. Thus, if K^w is not a cone of $\tilde{N}(M)$,

there are two nested sets $\mathcal{S}_1, \mathcal{S}_2$ so that $K_{\mathcal{S}_1}, K_{\mathcal{S}_2} \subseteq K^w$, and $\text{relint}(K_{\mathcal{S}_1} \cap K_{\mathcal{S}_2}) \subseteq \text{relint } K^w$. Let $w^1 \in \text{relint } K_{\mathcal{S}_1}$, and $w^2 \in \text{relint } K_{\mathcal{S}_1 \cap \mathcal{S}_2} = \text{relint}(K_{\mathcal{S}_1} \cap K_{\mathcal{S}_2})$. Since $w^1, w^2 \in \text{relint } K^w$, we have $\text{argmax}_{e \in C} w_e^1 = \text{argmax}_{e \in C} w_e^2$, for all circuits C of M .

Suppose for a contradiction that $\mathcal{S}_1 \neq (\mathcal{S}_1 \cap \mathcal{S}_2)$. Then there exists $F \in \mathcal{S}_1 \setminus (\mathcal{S}_1 \cap \mathcal{S}_2)$. As every nested set contains $[q]$, $\mathcal{S}_1 \cap \mathcal{S}_2$ is a non-empty nested set. Thus, there must exist some minimal $F' \in \mathcal{S}_1 \cap \mathcal{S}_2$ containing F . Note that as $F \notin \mathcal{S}_2$, we have the strict containment $F \subset F'$ and we can pick some $i \in F' \setminus F$.

We now define F_1, \dots, F_k to be the maximal flats in $\mathcal{S}_1 \cap \mathcal{S}_2$ which are contained in F . Note that as these flats are incomparable, the closure of their union cannot be connected (by the definition of nested sets). This closure must therefore be strictly contained in F , so we can pick some j in $F \setminus (F_1 \cup \dots \cup F_k)$.

The flat F' is connected, so there is some circuit $C \subset F'$ connecting i, j . We consider the argmax over this circuit. For $w^1 \in \text{relint } K_{\mathcal{S}_1}$, we have shown that:

$$\text{argmax}_{e \in C} w_e^1 = C \setminus \cup_{C \not\subset F'' \in \mathcal{S}^1} F'' \subseteq C \setminus F.$$

Hence $j \notin \text{argmax}_{e \in C} w_e^1$.

We now consider $\text{argmax}_{e \in C} w^2$ for $w^2 \in \text{relint } K_{\mathcal{S}_1 \cap \mathcal{S}_2}$. We claim there is no element of $\mathcal{S}_1 \cap \mathcal{S}_2$ that both contains j and does not contain C . If our claim holds, then

$$\text{argmax}_{e \in C} w_e^2 = C \setminus \cup_{C \not\subset F'' \in \mathcal{S}_1 \cap \mathcal{S}_2} F'' \ni j.$$

Therefore we have some circuit C such that $\text{argmax}_{e \in C} w_e^1 \neq \text{argmax}_{e \in C} w_e^2$, and this contradicts our assumption that $w^1, w^2 \in \text{relint } K^w$.

It therefore remains to prove our claim that there is no element of $\mathcal{S}_1 \cap \mathcal{S}_2$ that both contains j and does not contain C ; suppose for a contradiction that F'' is an element of $\mathcal{S}_1 \cap \mathcal{S}_2$ such that $C \not\subset F''$ and $j \in F''$. Then $F'' \subset F'$ as F'' has non-empty intersection with F' but doesn't contain all of C . Also, either $F \subset F''$ or $F'' \subset F$ as we have $j \in F \cap F''$. Since no flat satisfies $F \subset F'' \subset F'$, we must have $F'' \subset F$. But our choice of j ensures that $j \notin F''$; thus, no such F'' exists. Hence, for all F'' satisfying $C \not\subset F'' \in \mathcal{S}_1 \cap \mathcal{S}_2$, either $C \cap F'' = \emptyset$ or $j \notin F''$.

We have shown that the cones of the nested set fan and the argmax fan are in bijection. We conclude by noting that if w' is a point on the boundary of K^w , then $w \in K_{\mathcal{S}}$ and $w' \in K_{\mathcal{S}'}$, where $\mathcal{S}' \subseteq \mathcal{S}$. Therefore, $\text{argmax}_{e \in C} w'_e \subseteq \text{argmax}_{e \in C} w_e$ for all circuits C , and therefore $K^{w'} \subseteq K^w$. This completes the proof of (2). \square

When $M(K_p)$ is the matroid of the complete graph on p vertices, $\mathcal{U}_{M(K_p)}$ is the space of equidistant trees on p leaves (Ardila and Klivans 2006), or equivalently the space of ultrametrics \mathcal{U}_p . In this case, the coordinates of the ambient space, \mathbb{R}^q , correspond to the $q = \binom{p}{2}$ edges of the complete graph. Each cone of $\tilde{N}(M)$ corresponds to a unique tree topology on p leaves. This is why points in \mathcal{U}_M are referred to as M -ultrametrics. For general matroids, the fan structures $\tilde{\mathcal{B}}(M)$ and $\tilde{N}(M)$ may not coincide, as demonstrated in the following example.

Example 1 Let $M = M(G)$ be the rank $r = 5$ graphical matroid described by the graph G in Figure 1, which will serve as our running example. M has 30 bases, 6 circuits, and 78 (proper) flats. $\tilde{\mathcal{B}}(M)$ contains 54 maximal cones, 18 of which are further refined by $\tilde{N}(M)$, which contains 79 maximal cones. Further refinement is possible, e.g. via Rincon's *cyclic*

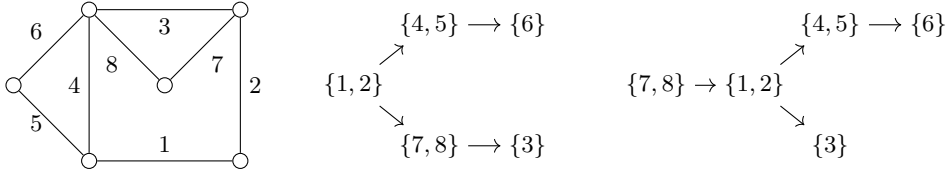


Fig. 1: Left: The graph G representing the graphical matroid $M(G)$ in [Example 1](#). Center: The nested set structure of the flats generating the maximal cone $K_{S_1} \in \tilde{N}(M)$. Right: The nested set structure for K_{S_2} .

Bergman fan ([Rincón 2013](#)), which contains 88 maximal cones and subdivides 9 maximal cones of $\tilde{N}(M)$.

Maximal cones of the Bergman fan $\tilde{B}(M)$ correspond to unordered partitions $\{B_1, \dots, B_r\}$ of $[q]$ into r non-empty blocks ([Feichtner and Sturmfels 2005](#), Corollary 4.7). Let $K \in \tilde{B}(M)$ be the cone identified by the partition $\{\{1, 2\}, \{3\}, \{4, 5\}, \{6\}, \{7, 8\}\}$. [Figure 1](#) depicts the two nested sets S_1 and S_2 of the partition, which refine K into $K_{S_1}, K_{S_2} \in \tilde{N}(M)$. Let $F_U := \{e_j \mid j \in U\}$ denote a flat of M . For $S_1 = \{F_3, F_6, F_{378}, F_{456}\}$, if we let $\mu = 5$, $\lambda_{F_3} = \lambda_{F_6} = \lambda_{F_{378}} = 2$, and $\lambda_{F_{456}} = 3$, then (1) yields the vector $w = (5, 5, 1, 2, 2, 0, 3, 3) \in \text{relint}(K_{S_1})$. The cone K_{S_1} is further refined into two maximal cones in the cyclic Bergman fan through F_{345678} , which is cyclic (see ([Rincón 2013](#))) but not connected.

We view the space of M -ultrametrics through the lens of tropical geometry. The *tropical max-plus semiring* is $\mathbb{T} := (\mathbb{R} \cup \{-\infty\}, \oplus, \odot)$, where $a \oplus b$ is defined as the maximum, $\max(a, b)$, and $a \odot b$ is given by the classical addition $a + b$. Tropical arithmetic extends coordinate-wise to the semimodule \mathbb{T}^q . The tropical sum of two vectors is their coordinate-wise maximum, and tropical scalar multiplication by $\lambda \in \mathbb{T}$ is translation by $\lambda \mathbf{1}$.

The $(q-1)$ -dimensional *tropical projective torus*, $\mathbb{R}^q/\mathbb{R}\mathbf{1}$, is a quotient space constructed by endowing \mathbb{R}^q with the equivalence relation $x \sim y \Leftrightarrow x = a \odot y$. Similarly, the $(q-1)$ -dimensional *tropical projective space* is $\mathbb{TP}^{q-1} = (\mathbb{T}^q \setminus \{-\infty\mathbf{1}\})/\mathbb{R}\mathbf{1}$. Going forward, we identify \mathcal{U}_M with its image in $\mathbb{R}^q/\mathbb{R}\mathbf{1}$; for the closure of \mathcal{U}_M in \mathbb{TP}^{q-1} , we use $\tilde{\mathcal{U}}_M$. This is justified by the fact that for any M -ultrametric w , $a \odot w$ is also an M -ultrametric for any $a \in \mathbb{T}$.

Ardila showed in ([Ardila 2004](#), Section 4) that $\tilde{\mathcal{U}}_M$ is a tropical polytope in \mathbb{TP}^{q-1} . A *tropical polytope* P is the set of all tropical linear combinations of points in a finite set $V \subseteq \mathbb{TP}^{q-1}$. If $V = \{v_1, \dots, v_r\}$, we denote this set by

$$\text{tconv}(V) = \{(\lambda_1 \odot v_1) \oplus \dots \oplus (\lambda_r \odot v_r) : \lambda_1, \dots, \lambda_r \in \mathbb{T}\}.$$

Proposition 4 (Section 4, ([Ardila 2004](#))) *The vertices of $\tilde{\mathcal{U}}_M$ as a tropical polytope are*

$$V_M = \{v_F : F \text{ is a maximal proper flat of } M\},$$

where $v_F \in \mathbb{TP}^{q-1}$ is the vector whose i^{th} coordinate is $-\infty$ if $i \in F$, and 0 otherwise.

We now consider the metric geometry of the tropical projective torus and Bergman fans. We endow the tropical projective torus with the *tropical metric*, which is given by

$$d_{\text{tr}}(x, y) = \max_{1 \leq i \leq q} \{y_i - x_i\} - \min_{1 \leq i \leq q} \{y_i - x_i\} = \max_{1 \leq i, j \leq q} \{x_i - y_i - x_j + y_j\} \quad (3)$$

for all $x, y \in \mathbb{R}^q / \mathbb{R}\mathbf{1}$.

[Develin and Sturmfels \(2004\)](#) give an explicit map, $\pi_P : \mathbb{TP}^{q-1} \rightarrow P$, which outputs a nearest point in P under the tropical metric. We recall that map now.

Definition 5 (Projection to a Tropical Polytope ([Develin and Sturmfels 2004](#))) *Let $P = \text{tconv}(v_1, \dots, v_r)$. For $i \in [r]$, define $\lambda_i = \max\{\lambda \in \mathbb{R} : \lambda \odot v_i \odot x = x\} = \min_e(x - v_i)_e$. For any $x \in \mathbb{TP}^{q-1}$, the point*

$$\pi_P(x) = (\lambda_1 \odot v_1) \oplus \dots \oplus (\lambda_r \odot v_r)$$

minimizes the distance $d_{\text{tr}}(y, x)$ over all $y \in P$. We call $\pi_P(x)$ the tropical projection to P .

The vertices of \mathcal{U}_M given in [Theorem 4](#), together with the tropical projection in [Theorem 5](#), define a map $\pi_{\tilde{\mathcal{U}}_M} : \mathbb{TP}^{q-1} \rightarrow \tilde{\mathcal{U}}_M$. Restricting the domain to $\mathbb{R}^q / \mathbb{R}\mathbf{1}$ yields a map $\pi_{\mathcal{U}_M} : \mathbb{R}^q / \mathbb{R}\mathbf{1} \rightarrow \mathcal{U}_M$, which we refer to by π_M to emphasize its dependency on the matroid M .

A particularly important fact that we will use about tropical projections is that they are non-expansive under the tropical metric. To our knowledge, this result first appeared in the preprint ([Jaggi et al. 2008](#)); we also include a short proof here.

Lemma 6 (Lemma 19, ([Jaggi et al. 2008](#))) *Let $\pi_M : \mathbb{R}^q / \mathbb{R}\mathbf{1} \rightarrow \mathcal{U}_M$ be the tropical projection to the space of M -ultrametrics. For all $x, y \in \mathbb{R}^q / \mathbb{R}\mathbf{1}$,*

$$d_{\text{tr}}(\pi_M(x), \pi_M(y)) \leq d_{\text{tr}}(x, y). \quad (4)$$

Proof Recall that V_M is the vertex set of \mathcal{U}_M as a tropical polytope ([Theorem 4](#)). Let λ_i^x, λ_i^y be the coefficients of $v_i \in V_M$ in the tropical expressions for $\pi_M(x), \pi_M(y)$. Fix vertices $v_k, v_l \in V_M$ such that $\pi_M(x)_j = \lambda_k^x + v_{kj} = \max_i \lambda_i^x + v_{ij}$ and $\pi_M(y)_j = \lambda_l^y + v_{lj} = \max_i \lambda_i^y + v_{ij}$. Then

$$\begin{aligned} \pi_M(x)_j - \pi_M(y)_j &= \lambda_k^x + v_{kj} - \lambda_l^y - v_{lj}, \\ &\geq \lambda_l^x + v_{lj} - \lambda_l^y - v_{lj}, \\ &\geq \min_e(x_e - v_{le}) - \min_f(y_f - v_{lf}), \\ &\geq \min_e(x_e - v_{le} - y_e + v_{le}), \\ &= \min_e(x_e - y_e). \end{aligned}$$

Similarly, we can show that:

$$\pi_M(x)_j - \pi_M(y)_j \leq \max_e(x_e - y_e).$$

Hence we conclude that $d_{\text{tr}}(\pi_M(x), \pi_M(y)) \leq d_{\text{tr}}(x, y)$. \square

2.3 Tropical Projection Safety Radius

Here we generalize the safety radius for phylogenetic reconstruction defined in (Atteson 1999) to the projection π_M to the Bergman fan of an arbitrary matroid. The classical safety radius measures how much a tree metric can be perturbed, assuming that the phylogenetic reconstruction method recovers the same tree topology. The topology of T is encoded by the cone of \mathcal{T}_p which contains D_T in its relative interior. Thus, the question is: for $w \in \mathcal{U}_M$, when is $\pi_M(w + \epsilon)$ contained in the relative interior of K^w ?

The tolerance for noise depends on how close the input $w \in \mathcal{U}_M$ is to the boundary of K^w . To measure this distance, we use the following notation. For a set U , the *first maximum* of U , denoted $\max^1 U$, is the usual maximum, while the *second maximum* of U , denoted $\max^2 U$, is the second greatest value in U . When we write $\max^i w$ for $w \in \mathbb{R}^q$, we mean the i^{th} maximum of the entries of w as a set. In particular, for non-constant w , $\max^1 w$ is always strictly greater than $\max^2 w$. Similarly, we use \min^i to denote the i^{th} minimum.

Lemma 7 *Let M be any matroid, and let K be a maximal cone in the nested set fan $\tilde{N}(M)$. For any $w \in \text{relint } K$, the tropical distance from w to the boundary ∂K is $w_{\min} := \min_C (\max_{e \in C} w_e - \max_{e \in C}^2 w_e)$, where this minimum is taken over all C such that $\max_{e \in C} w_e - \max_{e \in C}^2 w_e \neq 0$.*

As w is in the relative interior of a maximal cone, it is not the constant vector. We also know that M is connected, so there must be some circuit on which C is not constant. This ensures that w_{\min} is well defined and positive.

Proof Let u be any point in \mathcal{U}_M , and let K' be the cone of $\tilde{N}(M)$ containing u in its relative interior. Recall that $K \subseteq K'$ if and only if for all circuits C , $\text{argmax}_{e \in C} u_e \subseteq \text{argmax}_{e \in C} w_e$. Since K is a maximal cone, this is equivalent to $K = K'$.

We first show that if $d_{\text{tr}}(u, w) < w_{\min}$, then $u \in \text{relint } K$. We proceed by contradiction. Suppose there is a circuit C of M and an index $a \in [q]$ such that u_a is maximal for C , but w_a is not maximal for C . Let $b \in \text{argmax}_{e \in C} w_e$. As w is not constant on C , we have that

$$w_{\min} \leq \max_{e \in C}^1 w_e - \max_{e \in C}^2 w_e \leq w_b - w_a.$$

Since $d_{\text{tr}}(u, w) < w_{\min}$:

$$u_a - u_b < w_a - w_b + w_{\min} \leq w_a - w_b + (w_b - w_a) = 0.$$

This implies $u_a < u_b$, contradicting the maximality of u_a . Thus, we conclude $u \in \text{relint } K$.

It remains to show that there is some $u \in \partial K$ such that $d_{\text{tr}}(u, w) = w_{\min}$. We construct such a u explicitly. Define C to be a circuit of M such that $\max_{e \in C}^1 w_e - \max_{e \in C}^2 w_e = w_{\min}$, which exists as w is not constant and M is connected. Let B be the set of all indices $b \in [q]$ for which $w_b = \max_{e \in C}^2 w_e$. We define $u := w + w_{\min} \mathbf{1}_B$. For an example of this construction with equidistant trees, see Figure 2.

By construction, $d_{\text{tr}}(w, u) = w_{\min}$. We will now show that $u \in \partial K$. For each circuit C of M , we have four cases to consider:

1. $B \cap C = \emptyset$,
2. $B \cap C \neq \emptyset$, $\max_{e \in C} w_e \geq w_b + w_{\min}$,
3. $B \cap C \neq \emptyset$, $w_b < \max_{e \in C} w_e < w_b + w_{\min}$,

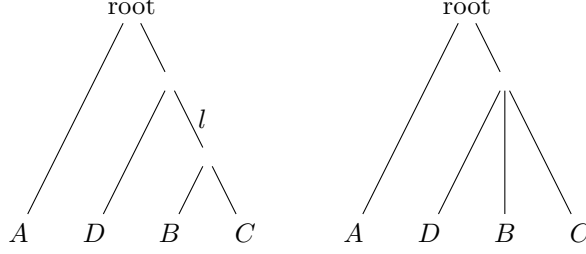


Fig. 2: When $M = M(K_p)$ is the matroid of the complete graph on p vertices, $w \in \mathcal{U}_M$ corresponds to an equidistant tree. When w is in the relative interior of a maximal cone of $\tilde{N}(M)$, the corresponding tree is binary, as exemplified by the tree on the left. In this case, the value w_{\min} is exactly the tree's minimal internal edge length, l . The right equidistant non-binary tree has metric u , which has tropical distance l from w , as constructed in the proof of [Theorem 7](#).

4. $B \cap C \neq \emptyset, w_b = \max_{e \in C} w_e$.

In case (1), $B \cap C = \emptyset$, and thus $u_e = w_e$ for all $e \in C$. In particular, that implies $\operatorname{argmax}_{e \in C} u_e = \operatorname{argmax}_{e \in C} w_e$. In case (2), $\max_{e \in C} w_e$ is unchanged, although more coordinates may achieve the maximum. Thus, $\operatorname{argmax}_{e \in C} u_e \supseteq \operatorname{argmax}_{e \in C} w_e$. Case (3) is not possible, since that would imply $w_{\min} > \max_{e \in C} w_e - w_b$, and that contradicts the definition of w_{\min} . Finally, in case (4), $B \cap C = \operatorname{argmax}_{e \in C} w_e$. Thus, the maximum increases: $\max_{e \in C} u_e = \max_{e \in C} w_e + w_{\min}$; but the coordinates achieving the maximum remain the same: $\operatorname{argmax}_{e \in C} u_e = \operatorname{argmax}_{e \in C} w_e$.

Hence, for every circuit we have $\operatorname{argmax}_{e \in C} u_e \supseteq \operatorname{argmax}_{e \in C} w_e$. Therefore, $u \in K$. However, for the circuit C' , the containment $\operatorname{argmax}_{e \in C'} u_e \supset \operatorname{argmax}_{e \in C'} w_e$ is strict, so $u \notin \operatorname{relint} K$. It follows that $u \in \partial K$. \square

[Theorem 7](#) motivates the following definition of safety radius for M -ultrametrics.

Definition 8 (Safety Radius) *Let $\pi_M : \mathbb{R}^q / \mathbb{R}\mathbf{1} \rightarrow \mathcal{U}_M$. The safety radius of π_M is the largest $s \in \mathbb{R}_{\geq 0}$ such that for every w in the relative interior of a maximal cone K of $\tilde{N}(M)$:*

$\pi_M(w + \epsilon)$ is in the relative interior of K for every $\epsilon \in (-sw_{\min}, sw_{\min})^q$,

where

$$w_{\min} = \min_C \left(\max_{e \in C}^1 w_e - \max_{e \in C}^2 w_e \right).$$

In introducing the safety radius of phylogenetic reconstruction methods, Atteson showed that the maximal possible safety radius is $1/2$ ([Atteson 1999](#)). Single-linkage has a safety radius of exactly $1/2$ ([Gascuel and McKenzie 2004](#)). Single-linkage coincides with $\pi_{M(K_p)}$ up to translation by $\mathbf{1}$ ([Ardila 2004](#)), so it is natural to extend their safety radius result to projections to general Bergman fans. This result follows directly from [Theorem 7](#).

Theorem 9 Let M be a matroid on a ground set with q elements. The safety radius of the tropical projection $\pi_M : \mathbb{R}^q/\mathbb{R}\mathbf{1} \rightarrow \mathcal{U}_M$ is $1/2$.

Proof Fix a point $w \in \mathcal{U}_M$, and let $v \in \mathbb{R}^q/\mathbb{R}\mathbf{1}$ and $s > 0$. Note that $d_{\text{tr}}(w, v) < 2sw_{\min}$ if and only if there exists $\epsilon \in (-sw_{\min}, sw_{\min})^q$ such that $w + \epsilon \sim v$. As π_M is a function of the equivalence classes of $\mathbb{R}^q/\mathbb{R}\mathbf{1}$, it therefore suffices to show that $1/2$ is the largest s such that $\pi_M(v)$ is in the relative interior of K for every v such that $d_{\text{tr}}(w, v) < 2sw_{\min}$.

If $s = 1/2$, then v satisfies $d_{\text{tr}}(w, v) < w_{\min}$, and by [Theorem 6](#) $d_{\text{tr}}(w, \pi_M(v)) < w_{\min}$. Together with [Theorem 7](#), this implies that $\pi_M(v) \in \text{relint } K$. On the other hand, by [Theorem 7](#), there are points on the boundary ∂K , which are exactly distance w_{\min} from w in the tropical metric. Therefore, we conclude that:

$$1/2 = \sup\{s : \forall \epsilon \in (-sw_{\min}, sw_{\min})^q, \pi_M(w + \epsilon) \in \text{relint } K\}. \quad \square$$

Example 2 We continue with $M = M(G)$, $K_{S_1} \subset K$, and $w \in \text{relint } K_{S_1}$ from [Example 1](#). Using [Theorem 8](#), we compute $w_{\min} = 2$. Suppose $\epsilon = 3/4(1, -1, -1, 1, 1, -1, -1, -1)$ and $w' = w + \epsilon$. Then $\pi_M(w') = 1/4(17, 17, 2, 11, 11, -3, 9, 9)$, which is still in $\text{relint } K_{S_1}$. If instead we consider the maximal cones of the cyclic Bergman fan, we find that $\pi_M(w')$ is contained in a different maximal cone than w . This is indicated by the flip from $w_4 < w_7$ in w to $w_4 > w_7$ in $\pi_M(w')$. Thus, w_{\min} depends on the how one elects to refine $\tilde{\mathcal{B}}(M)$.

3 Safety Radius for Fermat–Weber Points

In this section, we study the safety radius of an M -ultrametric estimate. An M -ultrametric estimate takes a sample from $\mathbb{R}^q/\mathbb{R}\mathbf{1}$ and outputs a single M -ultrametric or set of M -ultrametrics that summarize the data. We will consider the M -ultrametric estimate given by tropical projections of tropical Fermat–Weber points (see [Theorem 11](#)). The tropical projection is necessary because even for data in \mathcal{U}_M , the Fermat–Weber points of the data may lie outside of \mathcal{U}_M ([Lin et al. 2017](#); [Lin and Yoshida 2018](#)).

Definition 10 (Fermat–Weber function, Fermat–Weber points) For $S = \{v_1, \dots, v_n\} \subset X$, where X is a metric space with distance d , the corresponding Fermat–Weber function is

$$f_S(x) := \frac{1}{n} \sum_{i=1}^n d(x, v_i).$$

A Fermat–Weber point for S with respect to d is any point x^* minimizing the Fermat–Weber function on X :

$$x^* \in \underset{x \in X}{\operatorname{argmin}} f_S(x).$$

In general, Fermat–Weber points are not unique. Thus, we denote the set of all Fermat–Weber points of S by $\text{FW}(S) = \text{FW}(v_1, \dots, v_n)$.

We note that when d is the tropical metric, f_S is convex (in the classical sense) for any dataset $S \subset \mathbb{R}^q/\mathbb{R}\mathbf{1}$. We use the Fermat–Weber points under the tropical metric to define an M -ultrametric estimate.

Definition 11 A Fermat-Weber M -ultrametric point for data $v_1, \dots, v_n \in \mathbb{R}^q/\mathbb{R}\mathbf{1}$ is any point in $\pi_M(\text{FW}(v_1, \dots, v_n))$, where $\text{FW}(v_1, \dots, v_n)$ is taken with respect to the tropical metric. The method that computes $\pi_M(\text{FW}(v_1, \dots, v_n))$ is called the Fermat-Weber M -ultrametric method.

First, we will show that for a dataset $S \subset \mathcal{U}_M$, the intersection of $\text{FW}(S)$ with \mathcal{U}_M is exactly the projection of $\text{FW}(S)$ in $\mathbb{R}^q/\mathbb{R}\mathbf{1}$ onto \mathcal{U}_M .

Theorem 12 For any matroid M , and data $S = \{v_1, \dots, v_n\} \subset \mathcal{U}_M$, we have

$$\text{FW}(v_1, \dots, v_n) \cap \mathcal{U}_M = \pi_M(\text{FW}(v_1, \dots, v_n)). \quad (5)$$

In particular, $\text{FW}(v_1, \dots, v_n) \cap \mathcal{U}_M \neq \emptyset$.

Proof Note that every point in $\text{FW}(v_1, \dots, v_n) \cap \mathcal{U}_M$ is fixed under the projection π_M , and hence $\text{FW}(v_1, \dots, v_n) \cap \mathcal{U}_M \subseteq \pi_M(\text{FW}(v_1, \dots, v_n))$.

Next, we show that $\pi_M(\text{FW}(v_1, \dots, v_n))$ is contained in $\text{FW}(v_1, \dots, v_n) \cap \mathcal{U}_M$. For each $i = 1, \dots, n$:

$$d_{\text{tr}}(x, v_i) \geq d_{\text{tr}}(\pi_M(x), \pi_M(v_i)) = d_{\text{tr}}(\pi_M(x), v_i) \text{ for all } x \in \mathbb{R}^q/\mathbb{R}\mathbf{1}.$$

The inequality follows from the non-expansivity of π_M (Theorem 6), and the equality comes from the fact that $v_i \in \mathcal{U}_M$. Thus, $f_S(\pi_M(x)) \leq f_S(x)$. If x is a Fermat-Weber point of S , then $f_S(x)$ is already minimized, so $f_S(\pi_M(x)) = f_S(x) = \min_{y \in \mathbb{R}^q/\mathbb{R}\mathbf{1}} f_S(y)$. This means $\pi_M(x)$ is also a Fermat-Weber point. Hence, $\pi_M(\text{FW}(v_1, \dots, v_n)) \subseteq \text{FW}(v_1, \dots, v_n) \cap \mathcal{U}_M$.

The set of Fermat-Weber points is non-empty. Therefore, we have

$$\pi_M(\text{FW}(v_1, \dots, v_n)) = \text{FW}(v_1, \dots, v_n) \cap \mathcal{U}_M \neq \emptyset. \quad \square$$

This result enables us to compute the Fermat-Weber points in $\mathbb{R}^q/\mathbb{R}\mathbf{1}$, which is a classically convex optimization problem, and then project to \mathcal{U}_M , rather than optimizing f_S over the polyhedral fan \mathcal{U}_M . If $S \not\subset \mathcal{U}_M$, it is possible that $\text{FW}(S) \cap \mathcal{U}_M = \emptyset$, as Example 3 demonstrates. Thus, when $S \subset \mathcal{U}_M$ is perturbed by even a small amounts of noise, $\pi_M(\text{FW}(S + \epsilon)) \subseteq \text{FW}(S + \epsilon)$ may not hold.

Example 3 Let M be the matroid in our running example and $S = \{v_1, v_2, v_3\} \subset \mathcal{U}_M$ be given by the rows in the left matrix below.

$$S = \begin{pmatrix} 5 & 5 & 1 & 2 & 2 & 0 & 3 & 3 \\ 5 & 5 & 1 & 2 & 2 & 0 & 4 & 4 \\ 5 & 5 & 1 & 2 & 2 & 0 & 5 & 5 \end{pmatrix}, \quad S + \epsilon = \begin{pmatrix} 5 & 5 & 1.01 & 2 & 2.01 & -0.01 & 2.99 & 2.99 \\ 5.01 & 4.99 & 1 & 1.99 & 2.01 & 0 & 4 & 4 \\ 5.01 & 5 & 0.99 & 2.01 & 2 & 0 & 5 & 4.99 \end{pmatrix}$$

The unique tropical Fermat-Weber point of S is v_2 (Lin and Yoshida 2018, Lemma 8). Hence, $\pi_M(\text{FW}(S)) = \{v_2\}$. Let ϵ be such that $S + \epsilon = \{v'_1, v'_2, v'_3\}$ yields the matrix to the right where v'_i is the i^{th} row of the matrix. One can verify that $\text{FW}(S + \epsilon) = \{v'_2\}$ is also a singleton. As $v'_2 \notin \mathcal{U}_M$, we get $\pi_M(v'_2) = (4.99, 4.99, 1, 1.99, 1.99, 0, 4, 4) \neq v'_2$, which shows $\pi_M(\text{FW}(S + \epsilon)) \not\subseteq \text{FW}(S + \epsilon)$.

We now turn to computing the safety radius of the Fermat-Weber points, combined with a projection to \mathcal{U}_M . For the rest of the section, $S = \{v_1, \dots, v_n\} \subset \mathbb{R}^q/\mathbb{R}\mathbf{1}$. For noise vectors $\epsilon_1, \dots, \epsilon_n \in \mathbb{R}^q$, set $S + \epsilon := \{v_1 + \epsilon_1, \dots, v_n + \epsilon_n\}$.

Definition 13 (Fermat-Weber M -Ultrametric Safety Radius) *Fix a matroid M and a map $\pi_M : \mathbb{R}^q/\mathbb{R}\mathbf{1} \rightarrow \mathcal{U}_M$. The Fermat-Weber M -ultrametric projection method $S \mapsto \pi_M(\text{FW}(S))$ has a safety radius $s \in \mathbb{R}_{\geq 0}$ if, for any finite sample $S \subset \mathbb{R}^q/\mathbb{R}\mathbf{1}$, maximal cones K of $\tilde{N}(M)$, and $\epsilon_1, \dots, \epsilon_n \in \mathbb{R}^q$, the following holds:*

$$\text{if } \text{FW}(S) \cap \text{relint } K \neq \emptyset \text{ and } \sum_{j=1}^n \|\epsilon_j\|_{\text{tr}} < s \cdot \tilde{w}_{\min}, \text{ then } \pi_M(\text{FW}(S + \epsilon)) \cap \text{relint } K \neq \emptyset,$$

where $\tilde{w}_{\min} = \max_{w \in \pi_M(\text{FW}(S)) \cap K} w_{\min}$.

In what follows we will use \tilde{w} to denote a vector in $\pi_M(\text{FW}(S) \cap K)$ that achieves the maximum in the definition of \tilde{w}_{\min} .

The Fermat-Weber points of S are the minimizers (also known as M-estimators) for the *loss function* $f_S(x)$. For any loss function $f(x)$, we can compute the stability of a minimizer using a lower bound on the loss function $f(x)$ in terms of the distance from x to the set of minimizers (Hayashi 2000). The following lemma gives such a bound for the tropical Fermat-Weber function.

Lemma 14 *For any sample $S = \{v_1, \dots, v_n\} \subset \mathbb{R}^q/\mathbb{R}\mathbf{1}$, we have the following bound*

$$\frac{1}{n} d_{\text{tr}}(x, \text{FW}(S)) \leq f_S(x) - \min_{y \in \mathbb{R}^q/\mathbb{R}\mathbf{1}} f_S(y),$$

where $d_{\text{tr}}(x, \text{FW}(S)) = \min_{y \in \text{FW}(S)} d_{\text{tr}}(x, y)$.

Before proving [Theorem 14](#), we present a lemma which we use frequently.

Lemma 15 *For $U \subset [q]$, $x \in \mathbb{R}^q \setminus \mathbb{R}\mathbf{1}$ and all $0 < t < \max^1 x - \max^2 x$:*

$$\max_e(x + t\mathbf{1}_U)_e = \begin{cases} t + \max_e x_e & \text{if } U \cap \text{argmax}_e x_e \neq \emptyset, \\ \max_e x_e & \text{otherwise.} \end{cases}$$

Similarly, for all $0 < t < \min^2 x - \min^1 x$:

$$\min_e(x + t\mathbf{1}_U)_e = \begin{cases} t + \min_e x_e & \text{if } \text{argmin}_e x_e \subset U, \\ \min_e x_e & \text{otherwise.} \end{cases}$$

Proof We prove the result for $\max_e(x + t\mathbf{1}_U)_e$; the argument for $\min_e(x + t\mathbf{1}_U)_e$ is similar. Suppose $a \in U \cap \text{argmax}_e x_e$; then

$$(x + t\mathbf{1}_U)_a = t + x_a = t + \max_e x_e \geq \max_e(x + t\mathbf{1}_U)_e.$$

Hence $\max_e(x + t\mathbf{1}_U)_e = (x + t\mathbf{1}_U)_a = t + \max_e x_e$. Now suppose that $U \cap \text{argmax}_e x_e = \emptyset$. Then for all $a \in \text{argmax}_e x_e$, $(x + t\mathbf{1}_U)_a = x_a = \max_e x_e$. For $b \notin \text{argmax}_e x_e$:

$$(x + t\mathbf{1}_U)_b \leq t + x_b \leq t + x_a - (\max_e^1 x_e - \max_e^2 x_e) \leq x_a = (x + t\mathbf{1}_U)_a.$$

Hence $\max_e(x + t\mathbf{1}_U)_e = (x + t\mathbf{1}_U)_a = \max_e x_e$. \square

We can now prove [Theorem 14](#).

Proof To simplify the notation, we set $f(x) = f_S(x)$ throughout the proof. Fix $x \in \mathbb{R}^q/\mathbb{R}\mathbf{1}$, and let y be any point in $\text{FW}(S)$ which minimizes the tropical distance to x . The inequality in the lemma holds trivially for all $x \in \text{FW}(S)$, so let us assume $x \notin \text{FW}(S)$, and therefore $x \neq y$.

Let $d := d_{\text{tr}}(x, y) = d_{\text{tr}}(x, \text{FW}(S)) > 0$. Consider the tropical unit vector $(x - y)/d \in \mathbb{R}^q/\mathbb{R}\mathbf{1}$. The derivative of $f(y)$ in the $(x - y)/d$ direction is

$$\partial_{(x-y)/d} f(y) := \lim_{t \rightarrow 0^+} \frac{f(y + \frac{t}{d}(x - y)) - f(y)}{t}.$$

We will show that this directional derivative is bounded below by $1/n$:

$$1/n \leq \partial_{(x-y)/d} f(y). \quad (6)$$

As f is convex, $t^{-1}(f(y + \frac{t}{d}(x - y)) - f(y))$ does not increase as $t \rightarrow 0^+$. Thus, (6) implies that there is some sufficiently small t such that $1/n \leq t^{-1}(f(y + \frac{t}{d}(x - y)) - f(y))$. For such t , we have

$$\begin{aligned} \frac{1}{n} &\leq \frac{f(y + \frac{t}{d}(x - y)) - f(y)}{t} = \frac{f((1 - \frac{t}{d})y + \frac{t}{d}x) - f(y)}{t} \\ &\leq \frac{(1 - \frac{t}{d})f(y) + \frac{t}{d}f(x) - f(y)}{t} = \frac{1}{d}(f(x) - f(y)). \end{aligned}$$

The second inequality holds because f is convex. Clearing d from the denominators gives the inequality in the statement of the lemma. It therefore suffices to prove the inequality in (6).

To bound the derivative of $f(y)$ in the $(x - y)/d$ direction, we first consider directional derivatives in the direction of certain zero-one vectors. The tropical line segment from y to x is a concatenation of classical line segments ([Develin and Sturmfels 2004](#)). The number k of classical line segments in the tropical line segment from y to x is one less than the number of distinct entries in $x - y$. Let $\text{argmax}_a^j(x_a - y_a) \subseteq [q]$ be the coordinates of $x_a - y_a$ achieving the j th maximum. Then, the i^{th} line segment increases exactly the entries indexed by U_i , where $U_i := \bigcup_{1 \leq j \leq i} \text{argmax}_a^j(x_a - y_a) \subseteq [q]$. We note that

$$\begin{aligned} \emptyset &\subset U_1 \subset \cdots \subset U_k \subset [q], \\ \forall i : \text{argmin}_a(x_a - y_a) \cap U_i &= \emptyset, \\ \forall i : \text{argmax}_a(x_a - y_a) &\subset U_i. \end{aligned}$$

The i^{th} line segment is parallel to $u_i := \mathbf{1}_{U_i}$.

We will show that the directional derivatives $\partial_{u_i} f(y)$ are at least $1/n$.

Claim 1 For all u_i , the directional derivative of f at y in the direction of u_i satisfies

$$\frac{1}{n} \leq \partial_{u_i} f(y) := \lim_{t \rightarrow 0^+} \frac{f(y + tu_i) - f(y)}{t}.$$

Proof of Claim 1 As y minimizes f , we know $\partial_{u_i} f(y) \geq 0$. We will show $\partial_{u_i} f(y)$ is a positive integer multiple of $1/n$.

First we prove that $\partial_{u_i} f(y)$ is non-zero. Suppose for a contradiction that $\partial_{u_i} f(y)$ is zero. Since f is a piecewise linear function with finitely many pieces, for sufficiently small t , we have $f(y + tu_i) = f(y)$. Therefore, $y + tu_i$ is a Fermat-Weber point. Moreover, by [Theorem 15](#) and the definition of each U_i set, for sufficiently small t we have:

$$d_{\text{tr}}(x, y + tu_i) = \max_a (x_a - y_a - tu_{ia}) - \min_a (x_a - y_a - tu_{ia})$$

$$\begin{aligned}
&= \max_a(x_a - y_a - t) - \min_a(x_a - y_a - 0) \\
&< \max_a(x_a - y_a) - \min_a(x_a - y_a) \\
&= d_{\text{tr}}(x, y).
\end{aligned}$$

This contradicts the assumption that y is a closest Fermat-Weber point to x , so we conclude that $\partial_{u_i} f(y) \neq 0$.

Now writing out $\partial_{u_i} f(y)$ explicitly:

$$\begin{aligned}
\partial_{u_i} f(y) &= \lim_{t \rightarrow 0^+} \frac{1}{nt} \sum_{j=1}^n d_{\text{tr}}(y + tu_i, v_j) - d_{\text{tr}}(y, v_j) \\
&= \frac{1}{n} \sum_{j=1}^n \lim_{t \rightarrow 0^+} t^{-1} \\
&\quad \times \left[\max_a(y_a + tu_{ia} - v_{ja}) - \min_a(y_a + tu_{ia} - v_{ja}) - \max_a(y_a - v_{ja}) + \min_a(y_a - v_{ja}) \right].
\end{aligned}$$

If $y \not\sim v_j$, then let $t > 0$ be less than the smaller of $\max_a^1(y_a - v_a) - \max_a^2(y_a - v_a)$ and $\min_a^2(y_a - v_a) - \min_a^1(y_a - v_a)$. If $y \sim v_j$, then any t is sufficiently small. Then using [Theorem 15](#) for each i , we can expand $\max_a(y_a + tu_{ia} - v_{ja})$:

$$\max_a(y_a + tu_{ia} - v_{ja}) = \begin{cases} \max_a(y_a - v_{ja}) + t & U_i \cap \text{argmax}_a(y_a - v_{ja}) \neq \emptyset, \\ \max_a(y_a - v_{ja}) & U_i \cap \text{argmax}_a(y_a - v_{ja}) = \emptyset. \end{cases}$$

Similarly:

$$\min_a(y_a + tu_{ia} - v_{ja}) = \begin{cases} \min_a(y_a - v_{ja}) + t & \text{argmin}_a(y_a - v_{ja}) \subset U_i, \\ \min_a(y_a - v_{ja}) & \text{argmin}_a(y_a - v_{ja}) \not\subset U_i. \end{cases}$$

Hence, the summand of the directional derivative is

$$\begin{aligned}
&\lim_{t \rightarrow 0^+} t^{-1} (d_{\text{tr}}(y + tu_i, v_j) - d_{\text{tr}}(y, v_j)) \\
&= \lim_{t \rightarrow 0^+} t^{-1} \\
&\quad \times \left[\max_a(y_a + tu_{ia} - v_{ja}) - \min_a(y_a + tu_{ia} - v_{ja}) - \max_a(y_a - v_{ja}) + \min_a(y_a - v_{ja}) \right] \\
&= \begin{cases} 1 & U_i \cap \text{argmax}_a(y_a - v_{ja}) \neq \emptyset, \text{argmin}_a(y_a - v_{ja}) \not\subset U_i, \\ -1 & U_i \cap \text{argmax}_a(y_a - v_{ja}) = \emptyset, \text{argmin}_a(y_a - v_{ja}) \subset U_i, \\ 0 & \text{otherwise.} \end{cases}
\end{aligned}$$

These cases correspond to the cases where the maximum $\max_a(y_a + tu_{ia} - v_{ja})$ is increasing in t but the minimum $\min_a(y_a + tu_{ia} - v_{ja})$ is not, the minimum $\min_a(y_a + tu_{ia} - v_{ja})$ is increasing in t but the maximum $\max_a(y_a + tu_{ia} - v_{ja})$ is not, and the finally the case where they are either both increasing or both fixed in t . Hence the directional derivative $\partial_{u_i} f(y)$ is an integer multiple of $1/n$. We conclude that $\partial_{u_i} f(y) \geq 1/n$. \square

Next, we use the bounds on the directional derivatives $\partial_{u_i} f(y)$ to obtain the desired bound on $\partial_{(x-y)/d} f(y)$. We can write $x - y$ as a classical linear combination of u_1, \dots, u_k :

$$x - y = \mathbb{R}\mathbf{1} \odot \sum_{i=1}^k \gamma_i u_i,$$

where $\gamma_i = \max_a^i(x_a - y_a) - \max_a^{i+1}(x_a - y_a)$. Moreover, $\gamma_i > 0$ for all i , and $\sum_{i=1}^k \gamma_i = d_{\text{tr}}(x, y) = d$. This allows us to write $(x - y)/d$ as a convex combination of the u_i :

$$\frac{x - y}{d} = \mathbb{R}\mathbf{1} \odot \sum_{i=1}^k \lambda_i u_i, \quad (7)$$

where $\lambda_i = \gamma_i/d$ for $i = 1, \dots, k$; note that $\lambda_i > 0$, and $\sum_{i=1}^k \lambda_i = 1$.

Claim 2 Let $\lambda_1, \dots, \lambda_k \geq 0$, and $\sum_{i=1}^k \lambda_i = 1$. For sufficiently small t , $f(y + t \sum_i \lambda_i u_i) = \sum_i \lambda_i f(y + tu_i)$.

Proof of Claim 2 It suffices to consider a single term of the Fermat–Weber function, so we consider the distance to a single data point $v \in S$.

We must pick t small enough so that $\text{argmax}_a(y_a - v_a + t \sum_i \lambda_i u_{ia}) \subseteq \text{argmax}_a(y_a - v_a)$. We note that if $y = v$, then this holds for any t . Otherwise, as before, we require that $t < \max_a^1(y_a - v_a) - \max_a^2(y_a - v_a), \min_a^2(y_a - v_a) - \min_a^1(y_a - v_a)$. The distance to v is

$$d_{\text{tr}}(y + t \sum_i \lambda_i u_i, v) = \max_a(y_a - v_a + t \sum_i \lambda_i u_{ia}) - \min_a(y_a - v_a + t \sum_i \lambda_i u_{ia}).$$

We picked t small enough that any maximal coordinate for $y_a - v_a + t \sum_i \lambda_i u_{ia}$ must have also been maximal for $y_a - v_a$. Similarly, any minimal coordinate for $y_a - v_a + t \sum_i \lambda_i u_{ia}$ must also be minimal for $y_a - v_a$. This allows us to explicitly expand the maximum and minimum terms.

We first consider the maximum term in this distance. Consider $\text{argmax}_a(y_a - v_a) \cap U_i$ for $i = 1, \dots, k$. If $\text{argmax}_a(y_a - v_a) \cap U_i = \emptyset$ for all i , then by our choice of t , a perturbation by $t \sum_i \lambda_i u_{ia}$ leaves the maximum unchanged. Furthermore, since $\lambda_1 + \dots + \lambda_k = 1$, we have

$$\max_a(y_a - v_a + t \sum_i \lambda_i u_{ia}) = \max_a(y_a - v_a) = \sum_i \lambda_i \max_a(y_a - v_a + tu_{ia}).$$

Otherwise, let r be the smallest index such that $\text{argmax}_a(y_a - v_a) \cap U_r \neq \emptyset$. Then,

$$\begin{aligned} \max_a(y_a - v_a + t \sum_i \lambda_i u_{ia}) &= \max_a(y_a - v_a) + \sum_{i=r}^k \lambda_i t \\ &= \sum_{i=1}^{r-1} \lambda_i \max_a(y_a - v_a) + \sum_{i=r}^k \lambda_i (\max_a(y_a - v_a) + t) \\ &= \sum_{i=1}^k \lambda_i \max_a(y_a - v_a + tu_{ia}). \end{aligned}$$

We perform an analogous computation for the minimum term. Consider $\text{argmin}_a(y_a - v_a) \setminus U_i$ for $i = 1, \dots, k$. If $\text{argmin}_a(y_a - v_a) \setminus U_i$ is non-empty for all i , then the minimum remains unchanged and we can write:

$$\min_a(y_a - v_a + t \sum_i \lambda_i u_{ia}) = \min_a(y_a - v_a) = \sum_i \lambda_i \min_a(y_a - v_a + tu_{ia}).$$

Otherwise, let s be the smallest i such that $\text{argmin}_a(y_a - v_a) \setminus U_i = \emptyset$. Then,

$$\min_a(y_a - v_a + t \sum_{i=1}^k \lambda_i u_{ia}) = \min_a(y_a - v_a) + \sum_{i=s}^k \lambda_i t$$

$$\begin{aligned}
&= \sum_{i=1}^{s-1} \lambda_i \min_a (y_a - v_a) + \sum_{i=s}^k \lambda_i (\min_a (y_a - v_a) + t) \\
&= \sum_{i=1}^k \lambda_i \min_a (y_a - v_a + t u_{ia}).
\end{aligned}$$

So the claim holds for a single datapoint v , and by summing over our sample we get the desired result. \square

We can now compute the directional derivative $\partial_{(x-y)/d} f(y)$. Recall (7), which gives $(x-y)/d \odot \mathbb{R}\mathbf{1}$ as a convex combination of the u_i . We have

$$\begin{aligned}
\partial_{(x-y)/d} f(y) &= \lim_{t \rightarrow 0^+} \frac{f(y + t \sum_{i=1}^k \lambda_i u_i) - f(y)}{t} \\
&= \lim_{t \rightarrow 0^+} \frac{(\sum_{i=1}^k \lambda_i f(y + t u_i)) - (\sum_{i=1}^k \lambda_i) \cdot f(y)}{t} \\
&= \sum_{i=1}^k \lambda_i \lim_{t \rightarrow 0^+} \frac{f(y + t u_i) - f(y)}{t} = \sum_{i=1}^k \lambda_i \partial_{u_i} f(y).
\end{aligned}$$

Since $\partial_{u_i} f(y) \geq 1/n$ for all i , this implies $\partial_{(x-y)/d} f(y) \geq 1/n$. \square

Lemma 16 *Let $S = \{v_1, \dots, v_n\}$ be a sample in $\mathbb{R}^q/\mathbb{R}\mathbf{1}$, and let $S + \epsilon = \{v_1 + \epsilon_1, \dots, v_n + \epsilon_n\}$ for some $\epsilon_1, \dots, \epsilon_n \in \mathbb{R}^q$. Then,*

$$d_H(\text{FW}(S), \text{FW}(S + \epsilon)) \leq 2 \cdot \sum_{j=1}^n \|\epsilon_j\|_{\text{tr}},$$

where d_H is the Hausdorff distance using d_{tr} , which is given by:

$$d_H(A, B) = \max\{\sup_{x \in A} d_{\text{tr}}(x, B), \sup_{y \in B} d_{\text{tr}}(A, y)\}.$$

Proof We denote the Fermat-Weber functionals for the sample S and $S + \epsilon$ by f_S and $f_{S+\epsilon}$ respectively. Let y be any Fermat-Weber point of $S + \epsilon$. By Theorem 14, for all z in $\text{FW}(S)$:

$$\begin{aligned}
\frac{1}{n} d_{\text{tr}}(\text{FW}(S), y) &\leq f_S(y) - f_S(z) \\
&\leq f_S(y) - f_S(z) + f_{S+\epsilon}(z) - f_{S+\epsilon}(y) \\
&= \frac{1}{n} \sum_{j=1}^n d_{\text{tr}}(y, v_j) - d_{\text{tr}}(z, v_j) + d_{\text{tr}}(z, v_j + \epsilon_j) - d_{\text{tr}}(y, v_j + \epsilon_j).
\end{aligned}$$

The triangle inequality implies $d_{\text{tr}}(y, v_j) - d_{\text{tr}}(y, v_j + \epsilon_j) \leq d_{\text{tr}}(v_j, v_j + \epsilon_j)$, and also $d_{\text{tr}}(z, v_j + \epsilon_j) - d_{\text{tr}}(z, v_j) \leq d_{\text{tr}}(v_j, v_j + \epsilon_j)$. Thus,

$$\begin{aligned}
\frac{1}{n} d_{\text{tr}}(\text{FW}(S), y) &\leq \frac{1}{n} \sum_{j=1}^n 2 d_{\text{tr}}(v_j, v_j + \epsilon_j) \\
&= \frac{1}{n} \sum_{j=1}^n 2 \|\epsilon_j\|_{\text{tr}}.
\end{aligned}$$

Hence:

$$\sup_{y \in \text{FW}(S+\epsilon)} d_{\text{tr}}(\text{FW}(S), y) \leq 2 \sum_{j=1}^n \|\epsilon_j\|_{\text{tr}}.$$

A symmetrical argument proves that $\sup_{z \in \text{FW}(S)} d_{\text{tr}}(z, \text{FW}(S+\epsilon)) \leq 2 \sum_j \|\epsilon_j\|_{\text{tr}}$ as well. \square

This bound on $d_H(\text{FW}(S), \text{FW}(S+\epsilon))$ is not necessarily optimal for all n . For example, when $n=1$ the factor of two is superfluous. For a view of the empirical tightness of this bound, see [Figure A1](#).

Having identified concrete bounds on the stability of the tropical Fermat–Weber points, we can now state our main theorem.

Theorem 17 *For any matroid M , the Fermat–Weber M -ultrametric safety radius is $1/2$.*

Proof Let $S = \{v_1, \dots, v_n\}$ be a sample which has a tropical Fermat–Weber point in the relative interior of the cone $K \in \tilde{N}(M)$, and let w be the Fermat–Weber point in K that is furthest from the boundary of K , such that $\tilde{w}_{\min} = d_{\text{tr}}(w, \partial K)$. Suppose the sum of tropical norms of $\epsilon_1, \dots, \epsilon_n$ is at most $\tilde{w}_{\min}/2$. By [Theorem 16](#),

$$d_H(\text{FW}(S), \text{FW}(S+\epsilon)) \leq \tilde{w}_{\min}.$$

Therefore $S+\epsilon$ has some Fermat–Weber point u within \tilde{w}_{\min} of w , which ensures that $\pi_M(u)$ is also in $\text{relint } K$. \square

4 Stochastic Safety Radius and Experimental Results

The safety radius, as introduced by Atteson in ([Atteson 1999](#)), provides conditions for when a distance-based method returns a correct topology after introducing Gaussian noise to a tree metric. This definition of a safety radius is *deterministic* even though the input data are often multivariate random variables. This motivated Gascuel and Steel ([Gascuel and Steel 2016](#)) to define a “stochastic safety radius” in terms of a probability distribution: assuming the probability of returning the correct tree topology is at least $1 - \eta$, how much variation can our error have?

In this section, we extend the latter definition to Fermat–Weber M -ultrametric reconstructions for general matroids, showing that for any matroid and desired probability of success $1 - \eta$, there is some non-zero stochastic safety radius. In fact, for sufficiently large n, q , FW M -ultrametric stochastic safety radii can be taken arbitrarily close to $1/8$.

Definition 18 (FW M -Ultrametric Stochastic Safety Radius) *Fix a sample size n , a ground set $[q]$, and a matroid M on $[q]$. Some $s \in \mathbb{R}_{\geq 0}$ is a η -stochastic safety radius of the Fermat–Weber M -ultrametric method if, for any finite sample $S \subset \mathbb{R}^q / \mathbb{R}\mathbf{1}$, maximal cones K of $\tilde{N}(M)$, and i.i.d. random variables $\epsilon_1, \dots, \epsilon_n \sim N(0, \sigma^2 \mathbb{I}_q)$, the following holds:*

$$\text{FW}(S) \cap \text{relint } K \neq \emptyset \text{ and } \sigma < s \cdot \frac{\sqrt{2}\tilde{w}_{\min}}{n\sqrt{\log q}} \Rightarrow \mathbb{P}(\pi_M(\text{FW}(S+\epsilon)) \cap \text{relint } K \neq \emptyset) \geq 1 - \eta,$$

where $\tilde{w}_{\min} = \max_{w \in \pi_M(\text{FW}(S)) \cap K} w_{\min}$.

We note that in the standard phylogenetic stochastic safety radius, the coefficient of s depends on the number of leaves, p , instead of the dimension of the ambient space, $q = \binom{p}{2}$. However, for large leaf count p , $\sqrt{\log(q)} \approx \sqrt{2 \log(p)}$. This motivates the factor of $\sqrt{2}$ in our definition. Our definition is designed to standardize the order of magnitude of s for large n, q and to allow for a meaningful comparison between methods at different scales. This is reflected in the next theorem.

Theorem 19 *For any $\eta > 0$, $n, q \in \mathbb{N}$, and matroid M on $[q]$, there is a non-zero FW M -ultrametric stochastic safety radius $s > 0$. Moreover, the stochastic safety radius s can be taken arbitrarily close to $1/8$ for sufficiently large n, q .*

Proof We will use the notation from [Theorem 18](#). In particular, $\epsilon_1, \dots, \epsilon_n \sim N(0, \sigma^2 \mathbb{I}_q)$. By [Theorem 17](#), we have $\pi_M(\text{FW}(S + \epsilon)) \cap \text{relint } K$ is non-empty whenever $\text{FW}(S) \cap \text{relint } K \neq \emptyset$ and $\sum_{j=1}^n \|\epsilon_j\|_{\text{tr}} \leq \tilde{w}_{\min}/2$. Let $Z_1, \dots, Z_n \sim N(0, \mathbb{I}_q)$ be standard i.i.d. multivariate normal variables, so that $\epsilon_j \sim \sigma Z_j$, for $j = 1, \dots, n$. Define $E(q) = \mathbb{E}\|Z_j\|_{\text{tr}}$ and $V(q) = \text{Var}\|Z_j\|_{\text{tr}}$. Using Chebyshev's inequality:

$$\begin{aligned} \mathbb{P}(\pi_M(\text{FW}(S + \epsilon)) \cap \text{relint } K \neq \emptyset) &\geq \mathbb{P}\left(\sum_{j=1}^n \|\epsilon_j\|_{\text{tr}} \leq \frac{\tilde{w}_{\min}}{2}\right) \\ &= \mathbb{P}\left(\frac{1}{n} \sum_{j=1}^n \|Z_j\|_{\text{tr}} \leq \frac{\tilde{w}_{\min}}{2n\sigma}\right) \\ &= 1 - \mathbb{P}\left(\frac{1}{n} \sum_{j=1}^n \|Z_j\|_{\text{tr}} - E(q) > \frac{\tilde{w}_{\min}}{2n\sigma} - E(q)\right) \\ &\geq 1 - \mathbb{P}\left(\left|\frac{1}{n} \sum_{j=1}^n \|Z_j\|_{\text{tr}} - E(q)\right| > \frac{\tilde{w}_{\min}}{2n\sigma} - E(q)\right) \\ &\geq 1 - \frac{\text{Var}\left(\frac{1}{n} \sum_{j=1}^n \|Z_j\|_{\text{tr}}\right)}{(\tilde{w}_{\min}/(2n\sigma) - E(q))^2} \\ &= 1 - \frac{V(q)/n}{(\tilde{w}_{\min}/(2n\sigma) - E(q))^2}. \end{aligned}$$

Therefore, we know that $\mathbb{P}(\pi_M(\text{FW}(S + \epsilon)) \cap \text{relint } K \neq \emptyset) \geq 1 - \eta$ whenever the inequality $\eta \geq V(q)n^{-1}(\tilde{w}_{\min}/(2n\sigma) - E(q))^{-2}$ holds; this inequality holds for all σ such that

$$\sigma \leq \frac{\tilde{w}_{\min}}{2(nE(q) + \sqrt{nV(q)/\eta})}.$$

It therefore suffices to find s such that

$$s < \frac{\sqrt{\log q}}{2\sqrt{2}(E(q) + \sqrt{V(q)/n\eta})}.$$

$E(q), V(q) > 0$ all q , thus, there is some positive safety radius $s > 0$ for all n, q .

It is well known that for i.i.d. normal variables Z_{j1}, \dots, Z_{jq} , we have $\mathbb{E}[\max_l Z_{jl}]/\sqrt{\log q} \rightarrow \sqrt{2}$ as $q \rightarrow \infty$. Therefore, $E(q)/\sqrt{\log q} = 2\mathbb{E}[\max_l Z_{jl}]/\sqrt{\log q} \rightarrow 2\sqrt{2}$ as $q \rightarrow \infty$. Thus, for all $\eta, \delta > 0$, and sufficiently large n, q , we have η -stochastic safety radius $s > 1/8 - \delta$. \square

This result mirrors Proposition 2 of (Gascuel and Steel 2016), providing some theoretical intuition for the order of magnitude we might expect for s . [Theorem 19](#) provides a benchmark against which to compare safety radius estimates, but it is known to be hard to compute exact tight safety radii values in general. Rather, stochastic stability is best measured through computational simulation, which we now demonstrate.

Let M be the graphical matroid from our running example. We select a point v_0 from the relative interior of a randomly selected maximal cone $K \in \tilde{N}(M)$ such that $\|v_0\|_{\text{tr}} = 1$. Let $S = \{v_j \mid j \in [n]\} \subset \mathbb{R}^q$ be a sample of size n centered on v_0 . Here we sample via a multivariate Gaussian $v_j \sim \mathcal{N}(v_0, \mathbb{I}_q \sigma)$ with $\sigma = 3$ and $n = 25$, followed by a projection of the points to \mathcal{U}_M . Since we require $\{\text{FW}(S) \cap \text{relint } K\} \neq \emptyset$ for some $K \in \tilde{N}(M)$, we reject any sample S failing to do so. This explains the decision to project samples to \mathcal{U}_M . Projection ensures (via [Theorem 12](#)) that $S \cap \mathcal{U}_M \neq \emptyset$, which greatly improves the likelihood that $S \cap \text{relint } K \neq \emptyset$ for a maximal cone $K \in \tilde{N}(M)$. Thus, while projection here is not strictly necessary, we find that in practice it helps to reduce sampling rejection rates. We repeat this procedure as necessary, selecting a new v_0 for each sample, until we attain a collection of 1,000 such samples.

To any sample S with $\text{FW}(S) \cap \text{relint } K \neq \emptyset$ for a maximal cone $K \in \tilde{N}(M)$, we can apply noise of varying magnitude, and check whether $\{\pi_M(\text{FW}(S + \epsilon)) \cap \text{relint } K\} \neq \emptyset$. This general procedure is outlined in [Algorithm 1](#).

Algorithm 1 Determine if $\{\pi_M(\text{FW}(S + \epsilon)) \cap \text{relint } K\} \neq \emptyset$.

Input: A sample $S = \{v_1, \dots, v_n\} \subset \mathbb{R}^q / \mathbb{R}\mathbf{1}$ such that $W := \{\text{FW}(S) \cap \text{relint } K\}$ is non-empty for some maximal cone $K \in \tilde{N}(M)$. Noise variance σ_ϵ^2 .

Output: Total noise $\sum_j \|\epsilon_j\|_{\text{tr}}$, \tilde{w}_{\min} and (if possible) a point $x \in \text{FW}(S + \epsilon)$ satisfying $\pi_M(x) \in \text{relint } K$.

```

1: Compute  $\text{FW}(S)$ .
2: Compute  $\tilde{w}_{\min} := \max_{w \in W}(w_{\min})$  and  $\tilde{w} := \text{argmax}_{w \in W}(w_{\min})$ .
3: for  $j = 1, \dots, n$  do generate noise  $\epsilon_j \sim \mathcal{N}(0, (\tilde{w}_{\min} \sigma_\epsilon)^2)$ .
4: Compute  $P := \text{FW}(\{v_1 + \epsilon_1, \dots, v_n + \epsilon_n\})$ .
5: if  $\exists x \in P$  such that  $\pi_M(x) \in \text{relint } K$  then  $x^* \leftarrow x$ 
6: else  $x^* \leftarrow \emptyset$ 
return  $\tilde{w}_{\min}$ ,  $\sum_j \|\epsilon_j\|_{\text{tr}}$ , and  $x^*$ .
```

The non-trivial portions of [Algorithm 1](#) are Lines 1, 2, and 5. In Line 1 (and similarly in Line 4) we compute the Fermat–Weber set’s hyperplane representation using the linear programming outlined in ([Sabol et al. 2024](#)). To compute \tilde{w} in Line 2 we solve for the Chebyshev center of K (under the tropical norm) subject to additional feasibility constraints imposed by $\text{FW}(S)$. A linear program for this problem is feasible by the assumption $\text{FW}(S) \cap K \neq \emptyset$ and bounded by $\text{FW}(S)$. Its solution directly yields \tilde{w} and \tilde{w}_{\min} as optimal decision variables with $\tilde{w}_{\min} > 0$ if and only if $\text{FW}(S) \cap \text{relint } K \neq \emptyset$. In fact, this is precisely the computation we perform when deciding whether to accept or reject a sample generated in the manner described in the previous paragraph. In other words, we compute Lines 1-2 when generating our samples.

After applying noise in Line 3, the points of the perturbed sample $S + \epsilon$ are not M -ultrametrics, even if $S \subset \mathcal{U}_M$ originally. Thus, we cannot leverage [Theorem 12](#) in evaluating Line 5. Instead, we compute the preimage of K under π_M and check if $\{\text{FW}(S + \epsilon) \cap \pi_M^{-1}(K)\}$ is nonempty. The preimage of K is a union of polyhedral cones, each of which arises by resolving disjunctive inequalities associated to the set of partial orders encoded in the nested set structure of K . For example, from [Figure 1](#) we see that the nested set structure for K_{S_1} requires $\min\{x_1, x_2\} \geq \min\{x_4, x_5\}, \min\{x_7, x_8\}$. Thus, $\pi_M^{-1}(K_{S_1})$ is the union of the four polyhedral cones whose associated half-spaces differ according to the four possible ways to assign minima on the right-hand side of the preceding inequality. By enumerating these preimage cones, we can perform a sequence of constrained Chebyshev center linear programs over each of them in turn, stopping if we encounter a feasible solution with positive objective function value. Such a solution x provides $x^* = \pi_M(x)$ in Line 5. If no such x is found after checking all cones in the preimage set, we conclude $\{\pi_M(\text{FW}(S + \epsilon)) \cap \text{relint } K\}$ is empty.

The next two examples demonstrate the empirical tightness of the bound given in [Theorem 16](#) and the Fermat–Weber M -ultrametric stochastic safety radius. Both examples use the matroid M from our running example and 1,000 samples of size $n = 25$ that are generated in the manner described earlier.

Example 4 To each of 1,000 samples S , we apply uniform noise ϵ scaled so that $\sum_j \|\epsilon_j\|_{\text{tr}} \approx \tilde{w}_{\min}/2$. That is, we apply noise that meets the threshold stipulated by our bound in [Theorem 17](#). Next, we compute the Fermat–Weber polytrope $P = \text{FW}(S + \epsilon)$, project \tilde{w} onto P , and then measure $d_{\text{tr}}(\tilde{w}, \pi_P(\tilde{w}))$. The tropical vertices of P used for the projection can be computed by solving a network flow problem (see [\(Sabol et al. 2024\)](#)). [Figure 3](#) (left) plots these 1,000 distances by the value of \tilde{w}_{\min} with the red dotted line indicating the bound given by [Theorem 16](#), offering some insight into its empirical tightness.

Example 5 Using the same 1,000 samples as in [Example 4](#), we execute [Algorithm 1](#) once for each noise level $\sigma_\epsilon \in \{1/32, 1/16, 1/8, 1/4, 1/2, 1, 2, 3, 4, 5\}$. At each iteration we record $\sum_{j=1}^n \|\epsilon_j\|_{\text{tr}}$ and whether $\pi_M(\text{FW}(S + \epsilon)) \cap \text{relint } K \neq \emptyset$. The results of the 10,000 trials are depicted in [Figure 3](#) (right) where the vertical dashed line indicates the noise threshold ratio provided in [Theorem 17](#). It is evident in this demonstration that the bound is extremely conservative, which is line with the observations made in [\(Gascuel and Steel 2016\)](#) for phylogenetic trees.

In order to determine how closely the results of [Example 5](#) match with other matroids on the same ground set, we repeat [Example 5](#) for all loopless, connected matroids on 8 elements with rank $r(M) \geq 2$. For this we use the matroid database in SAGEMATH ([The Sage Developers 2022](#)) to enumerate all matroids on [8]. After filtering out those we wish to exclude, we are left with 1,151 matroids. For expediency, we reduce the number of samples per matroid from 1,000 down to 10 while keeping the sample size $n = 25$ the same. Additionally, we apply noise only at $\sigma_\epsilon \in \{1/32, 1/8, 1, 3, 5\}$. The resulting 57,550 trials are depicted in [Figure 4](#) where we plot the x -axis on a log scale to better highlight the outcomes for small σ .

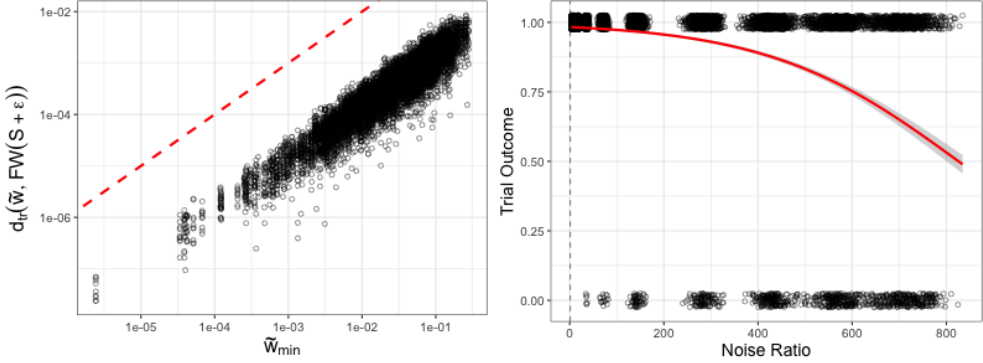


Fig. 3: Left: Tropical distances between \tilde{w} and $\text{FW}(S + \epsilon)$ after applying noise at the threshold given by [Theorem 17](#). Using 1,000 separate samples, we apply uniform noise proportionally scaled to achieve $\sum_j \|\epsilon_j\|_{\text{tr}} \approx \tilde{w}_{\min}/2$. We write approximately only to account for floating point precision in the computations. The red dashed line indicates the upper-bound on the Hausdorff distance given in [Theorem 16](#). We plot the results in log-log coordinates for better readability.

Right: Results for 10,000 applications of [Algorithm 1](#) using the same samples as in [Example 4](#). An outcome of 0 indicates $\pi_M(\text{FW}(S + \epsilon)) \cap \text{relint } K = \emptyset$. To each of the 1,000 separate samples we apply Gaussian noise according to 10 different progressively increasing variances so that we have 10 tests per sample. We plot the x-axis using the ratio of $\sum_j \|\epsilon_j\|_{\text{tr}} / (\tilde{w}_{\min}/2)$ to help normalize across samples. The vertical dashed line at $x = 1$ corresponds to the threshold of this ratio required in [Theorem 17](#). A logistic regression (red curve) with standard errors (gray bands) is added to show the overarching trend.

5 Conclusions

In this paper we explore the stability of projection to the space of M -ultrametrics for Fermat-Weber sets under additive noise. We extend several known results for the specific case of phylogenetic trees to the more general setting of arbitrary matroids. Our definitions (and proofs) utilize w_{\min} based on the nested set fan under a minimal building set, but the concepts apply equally to any refinement of the Bergman fan with an appropriate update to the formula given in [Theorem 8](#). Our empirical results suggest that the FW M-ultrametric safety radius is very conservative, which was expected given that the ultrametric safety radius is known to be extremely conservative in the case of phylogenetic trees. In future work, it would be interesting to find a tighter bound.

Acknowledgments. The authors thank to Yue Ren and Connor Simpson for useful conversations, and the anonymous reviewers for their comments. RY and JS are partially supported by NSF Statistics Program DMS 2409819. RT receives partial funding from a Technical University of Munich–Imperial College London Joint Academy of Doctoral Studies (JADS) award (2021 cohort, PIs Drton/Monod). SC, RT and RY are grateful to Jane Coons for bringing us together at the University of Oxford during the Workshop for Women in Algebraic Statistics in July 2024 supported by St John’s

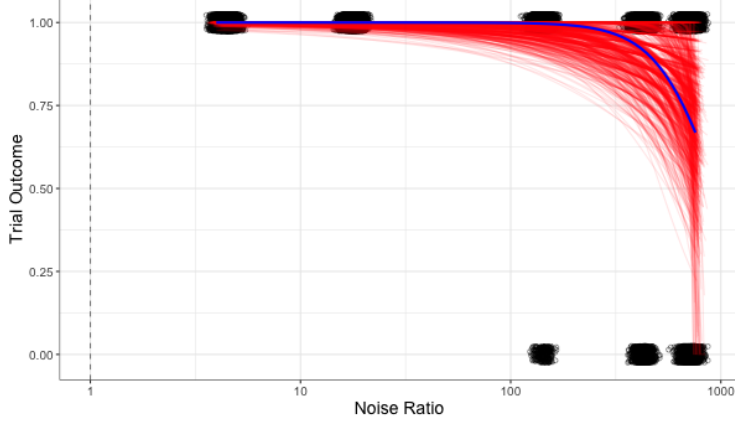


Fig. 4: We repeat [Example 5](#) for all loopless, connected matroids on 8 elements with rank $r(M) \geq 2$. For each matroid we construct 10 samples and vary $\sigma_\epsilon \in \{1/32, 1/8, 1, 3, 5\}$. Each red curve is a logistic regression for the experimental outcomes of a different matroid. The blue curve corresponds to the matroid from our running example. We plot the x -axis on a log scale to better depict results σ closer to the noise threshold (vertical dashed line at $x = 1$).

College, Oxford, the L’Oreal-UNESCO For Women in Science UK and Ireland Rising Talent Award in Mathematics and Computer Science (awarded to Jane Coons), the Heilbronn Institute for Mathematical Research, and the UKRI/EPSRC Additional Funding Programme for the Mathematical Sciences.

Appendix A Additional Computational Results

To study the empirical tightness of the bound on $d_H(\text{FW}(S), \text{FW}(S + \epsilon))$ given by [Theorem 16](#), we generate a random sample $S = \{v_1, \dots, v_n\}$, where each v_j drawn uniformly from the q -dimensional unit cube. To each v_j we add standard Gaussian noise $\epsilon_j \sim \mathcal{N}(0, \mathbb{I}_q)$, where \mathbb{I} is the $q \times q$ identity matrix. We compute $P = \text{FW}(S)$ and $P' = \text{FW}(S + \epsilon)$, and for each vertex $p \in P$ we compute $d_{\text{tr}}(p, \pi_{P'}(p))$. We perform similar computations for $d_{\text{tr}}(p', \pi_P(p'))$ and then take the maximum over all such distances to attain $d_H(\text{FW}(S), \text{FW}(S + \epsilon))$. We repeat this procedure 1,000 times for multiple values of n, q , and for each iteration, compute the *scaled shift*:

$$d_H(\text{FW}(S), \text{FW}(S + \epsilon)) / (\sum_j \|\epsilon_j\|_{\text{tr}}).$$

Results are depicted in [Figure A1](#). We note that in all trials, the scaled shift (x -axis) never exceeds a value of one, and the highest values are attained when $n = 2$. We also observe that scaled shift values generally decrease as a sample size increases. This suggests that it may be possible to modify the factor of two included in [Theorem 16](#) to incorporate information on a sample size so as to achieve tighter bounds.

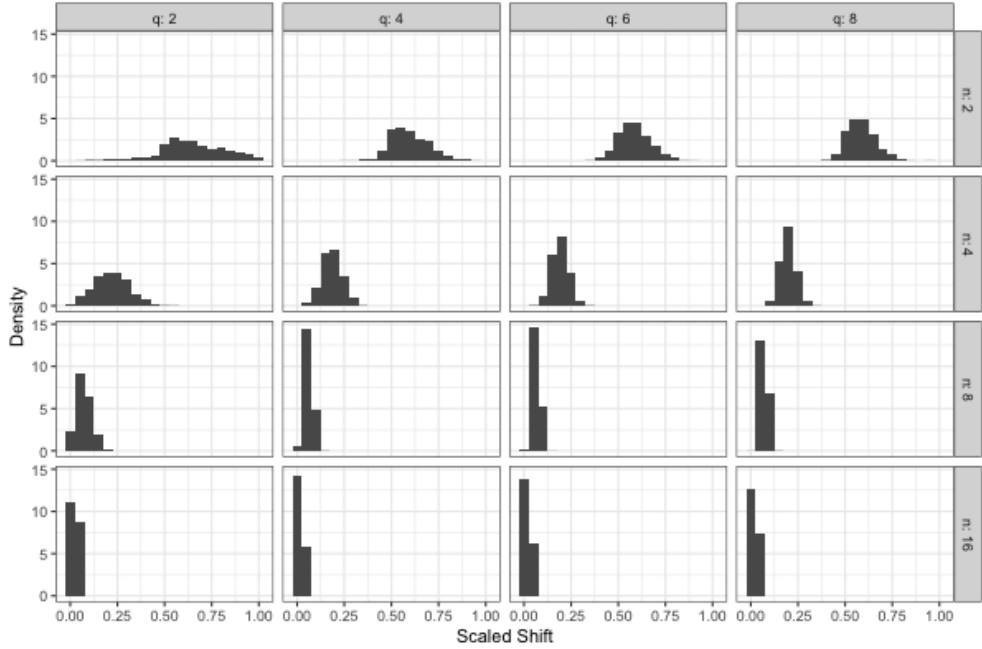


Fig. A1: Each histogram records the scaled shifts for 1,000 q -dimensional samples of n points, for $q = 2, 4, 6, 8$ and $n = 2, 4, 8, 16$. The 1,000 independent samples and perturbations are generated according to the procedure described in Appendix A.

References

Ardila F (2004) Subdominant matroid ultrametrics. *Ann Comb* 8(4):379–389. <https://doi.org/10.1007/s00026-004-0227-1>

Ardila F, Klivans CJ (2006) The Bergman complex of a matroid and phylogenetic trees. *J Combin Theory Ser B* 96(1):38–49. <https://doi.org/10.1016/j.jctb.2005.06.004>

Atteson K (1999) The performance of neighbor-joining methods of phylogenetic reconstruction. *Algorithmica* 25(2-3):251–278. <https://doi.org/10.1007/PL00008277>

Bernstein DI (2020) L -infinity optimization to Bergman fans of matroids with an application to phylogenetics. *SIAM J Discrete Math* 34(1):701–720. <https://doi.org/10.1137/18M1218741>

Buneman P (1974) A note on the metric properties of trees. *J Combinatorial Theory Ser B* 17(1):48–50. [https://doi.org/10.1016/0095-8956\(74\)90047-1](https://doi.org/10.1016/0095-8956(74)90047-1)

Develin M, Sturmfels B (2004) Tropical convexity. *Doc Math* 9:1–27. <https://doi.org/10.4171/dm/154>

Dress A, Holland B, Huber KT, et al (2005) Δ additive and Δ ultra-additive maps, Gromov’s trees, and the Farris transform. *Discrete Appl Math* 146(1):51–73. <https://doi.org/10.1016/j.dam.2003.01.003>

Dress AWM, Huber KT, Steel M (2014) A matroid associated with a phylogenetic tree. *Discrete Math Theor Comput Sci* 16(2):41–55. <https://doi.org/10.46298/dmtcs.2078>

Feichtner EM, Sturmfels B (2005) Matroid polytopes, nested sets and Bergman fans. *Port Math (NS)* 62(4):437–468. URL <http://eudml.org/doc/52519>

Gascuel O, McKenzie A (2004) Performance analysis of hierarchical clustering algorithms. *J Classification* 21(1):3–18. <https://doi.org/10.1007/s00357-004-0003-2>

Gascuel O, Steel M (2016) A ‘stochastic safety radius’ for distance-based tree reconstruction. *Algorithmica* 74(4):1386–1403. <https://doi.org/10.1007/s00453-015-0005-y>

Hayashi F (2000) *Econometrics*. Princeton University Press, Princeton, NJ

Jaggi M, Katz G, Wagner U (2008) New results in tropical discrete geometry. Preprint. URL <https://www.m8j.net/math/TropicalDiscreteGeometry.pdf>

Joswig M (2021) Essentials of tropical combinatorics, *Graduate Studies in Mathematics*, vol 219. American Mathematical Society, Providence, RI, <https://doi.org/10.1090/gsm/219>

Lin B, Yoshida R (2018) Tropical Fermat-Weber points. *SIAM J Discrete Math* 32(2):1229–1245. <https://doi.org/10.1137/16M1071122>

Lin B, Sturmfels B, Tang X, et al (2017) Convexity in tree spaces. *SIAM J Discrete Math* 31(3):2015–2038. <https://doi.org/10.1137/16M1079841>

Rincón F (2013) Computing tropical linear spaces. *J Symbolic Comput* 51:86–98. <https://doi.org/10.1016/j.jsc.2012.03.008>

Sabol J, Barnhill D, Yoshida R, et al (2024) Tropical polytropes. URL <https://arxiv.org/pdf/2402.14287.pdf>

Semple C, Steel M (2003) *Phylogenetics*, Oxford Lecture Series in Mathematics and its Applications, vol 24. Oxford University Press, Oxford, Oxford, UK, <https://doi.org/10.1093/oso/9780198509424.001.0001>

The Sage Developers (2022) SageMath, the Sage Mathematics Software System. URL <https://www.sagemath.org>